CLOT KINETICS IN THE PROGRESSION OF CEREBRAL VASOSPASM

A Thesis

by

ERIN KATHLEEN HACKNEY

Submitted to the Office of Graduate Studies of
Texas A&M University
in partial fulfillment of the requirements for the degree of

MASTER OF SCIENCE

December 2009

Major Subject: Biomedical Engineering

CLOT KINETICS IN THE PROGRESSION OF CEREBRAL VASOSPASM

A Thesis

by

ERIN KATHLEEN HACKNEY

Submitted to the Office of Graduate Studies of
Texas A&M University
in partial fulfillment of the requirements for the degree of

MASTER OF SCIENCE

Approved by:

Chair of Committee,	Jay D. Humphrey
Committee Members,	Duncan J. Maitland
	Emily Wilson
Head of Department,	Gerard L. Cote

December 2009

Major Subject: Biomedical Engineering

ABSTRACT

Clot Kinetics in the Progression of Cerebral Vasospasm. (December 2009)

Erin Kathleen Hackney, B.S., Texas A&M University

Chair of Advisory Committee: Dr. Jay D. Humphrey

Cerebral vasospasm following subarachnoid hemorrhage has high morbidity and mortality. Mathematical modeling of the progression of the condition provides insight to improve clinical treatment of patients post subarachnoid hemorrhage.

An existing model of the clotting cascade is expanded to include the theoretical conditions of cerebral vasospasm. We consider clotting factor XIIIa, which has been implicated as a primary cause of the entrenchment of the smaller diameter. Solutions for clotting are used as boundary conditions to solve the concentration of diffusible clotting factors in the vessel wall and cerebrospinal fluid (CSF).

Each domain (clot, vessel wall, CSF) is described by a separate initial-boundary value problem, requiring unique conditions, reaction-diffusion equations, and diffusion coefficients. Additionally, the results from the first domain (the clot) provide a subset of the boundary conditions for the second and third domains (arterial wall and CSF, respectively).

Although this approach captures many detailed components of the clotting process, a simpler method for investigating the formation and dissolution of a clot post subarachnoid hemorrhage is to neglect the bulk of the clot cascade to focus on the most

salient features, namely, the formation of cross-linked fibrin and the degradation of fibrin by plasmin. By assuming first order kinetics in the initial hours following hemorrhage, we find a simplified expression with kinetic rates that may be adjusted depending on experimental conditions.

TABLE OF CONTENTS

Page

LIST OF FIGURES

LIST OF TABLES

1. INTRODUCTION

Rupture of an intracranial aneurysm leading to subarachnoid hemorrhage (SAH) is the cause of 7% of all strokes (Liu-Deryke and Rhoney, 2006). Vasoactive molecules released by the clotting and inflammatory processes cause vasoconstriction in nearby arteries within 3 to 4 days following SAH and entrenchment of the smaller lumen diameter in 5 to 7 days (Liu-Deryke and Rhoney, 2006). This progression is referred to as cerebral vasospasm and occurs in 70% of SAH cases. Cerebral vasospasm causes symptomatic ischemia of brain tissue in 36% of SAH cases and increases mortality by 1.5 to 3 times (Komotar et al., 2007). There are no recognized treatments to prevent cerebral vasospasm, and the progression of the condition is not well understood.

The products of the formation and dissolution of the clot are important contributors to the progression of cerebral vasospasm. Patient outcome is predicted by clot clearance rate and clot density (Reilly et al., 2004; Rosen et al., 2007). Following the rupture of an aneurysm, blood exits the non-thrombogenic environment of the artery, activating platelets and initiating the clotting cascade, a series of biochemical reactions with multiple feedback loops. Additionally, the astrocytes and neurons respond to the inflammatory process by releasing additional vasoactive molecules. Numerous molecules have been implicated in the progression of cerebral vasospasm (Table 1), although no definitive list of key molecules has been identified to improve clinical treatment following subarachnoid hemorrhage.

Cerebral vasospasm may be the result of prolonged vasoconstriction, during

---

This thesis follows the style of Journal of Theoretical Biology.

which cellular and structural components re-orient in response to the altered mechanical environment, entrenching the smaller diameter. It has been shown that arterial exposure to norepinephrine for four hours induces inward eutrophic remodeling in rat cremaster muscle arteries (Martinez-Lemus et al., 2004). Martinez-Lemus et al. suggested that "in response to prolonged constriction, VSMCs undergo a mechanoadaptation process involving 'length autoregulation' that would be energetically favorable for maintenance of a reduced diameter and may provide a mechanism for the development of eutrophic remodeling of the vascular wall" (Martinez-Lemus et al., 2004).

Table 1
Species which have been suggested as potential culprits in the progression of cerebral vasospasm.

species	source	effect on wall structures	references
ET-1	endothelial cells and astrocytes	SMC constriction	Fassbender et al., 2000
thrombin	blood plasma	SMC proliferation; fibroblast proliferation	Bar-Shavit et al., 1990
transglutaminase (factor XIIIa & tTG)	blood plasma and platelets	cross-linking of ECM	Bakker et al., 2005 Langille and Dajnowjec, 2005
TGF-beta	platelets	increased matrix production	Flood et al., 2001
PDGF-AB	platelets	increased SMC proliferation	Zimmermann et al., 2005
bilirubin oxidation products	lysed red blood cells	SMC constriction	Clark and Sharp, 2006 Pyne-Geithman et al., 2005

Here we develop a theoretical framework for a mathematical model which describes the time course of the exposure of the arterial wall to vasoactive substances. An accurate model may indicate which molecules are of particular importance in cerebral vasospasm, allowing clinicians to identify more targeted treatments. We extend an existing model (Anand et al., 2008) to describe reaction-diffusion kinetics in the cerebrospinal fluid (CSF), clot, and arterial wall and include additional steps of the cross-linking of fibrin by activated factor XIII and fibrinolysis.

1.1 Clotting

Clotting is described by an enzymatic cascade (Figure 1). The intrinsic pathway is initiated by contact with damaged vascular tissue, bacteria, or a negatively charged surface. The more rapid extrinsic pathway is initiated following trauma by contact with tissue factor, which is produced by non-endothelial tissues. The extrinsic pathway accounts for the primary source of clotting following subarachnoid hemorrhage. The factor VIIa-tissue factor complex activates factor X. Prothrombinase is produced from activated factors V and X, allowing the conversion of prothrombin to thrombin.

Fibrin, a 340 kD plasma protein, provides the scaffolding of a mature clot (Blomback, 1996). Fibrin is formed from the zymogen fibrinogen by the removal of fibrinopeptide A and fibrinopeptide B by thrombin (Blomback, 1996). Tracking the appearance of these molecules allows for a description of the rate at which fibrin is produced. Alternatively, progression of clot formation can be tracked by monitoring the turbidity, or cloudiness, of the clot, which is related to the size of the fibrin fibers (Weisel and Nagaswami, 1992). Fibrin is ultimately degraded by plasmin, which cleaves the molecule through the process of fibrinolysis, resulting in fibrin degradation products (FDPs).

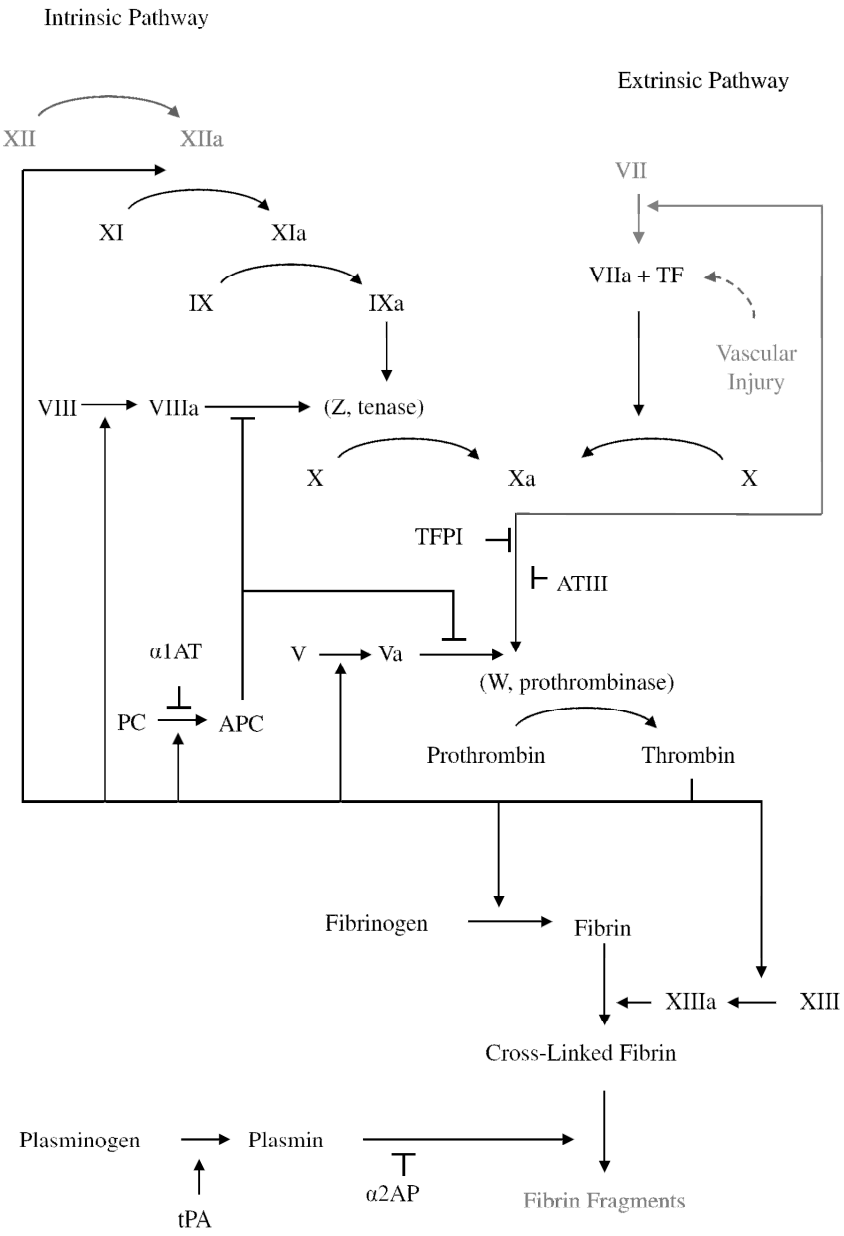

Figure 1
Schema of the clotting cascade. Lines with a bar indicate inhibitory action. Factors in gray are not included in the model proposed here.

Researchers have attempted to model clot kinetics since the clotting cascade was suggested in 1964 by Macfarlane (Macfarlane, 1964). Some have focused on individual steps of activation (Guy et al., 2007; Gir et al., 1996; Nesheim et al., 1992; Weisel and Nagaswami, 1992; Ataullakhanov et al., 2002). Others have summarized the major contributing species of the entire cascade (Baldwin and Basmadjian, 1994; Hockin et al., 2002; Khanin and Semenov, 1998; Anand et al., 2003; Anand et al., 2008). Additionally, some groups focus on in vitro clotting (Anand et al., 2008; Weisel and Nagaswami, 1992), while others are concerned with in vivo situations (Anand, 2004; Swaminathan, 2004; Guy et al., 2006).

2. MODEL DEVELOPMENT

We extend an existing model to include a potentially important clotting factor, Factor XIIIa, and to include the diffusion of clot factors into the vessel wall and CSF. We first give a brief explanation of the Anand model and continue with the development of the theoretical framework for the proposed model. Figure 2 is a schema of how the Anand model applies to the problem of cerebral vasospasm, and Figure 3 illustrates how it might be extended to provide clinical insight. A summary of the components necessary to complete a well-posed problem for each domain is provided in Appendix B.

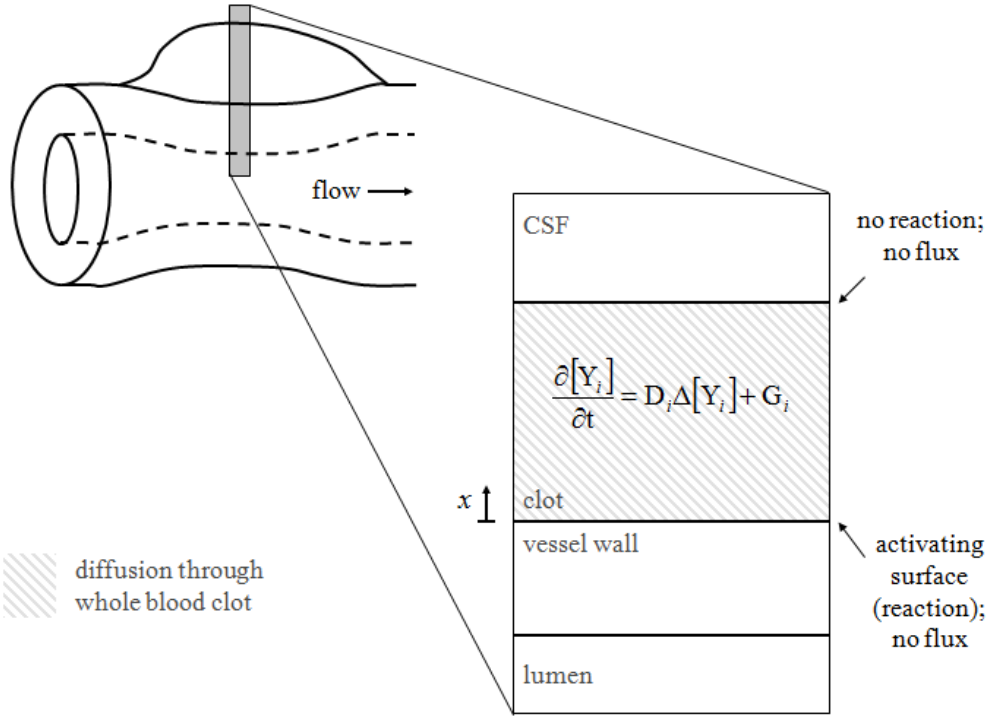

Figure 2
Schema of the existing model (Anand et al., 2008), describing reaction and diffusion through the clot with no diffusion of products into the vessel wall or CSF. i = 1,…,27.

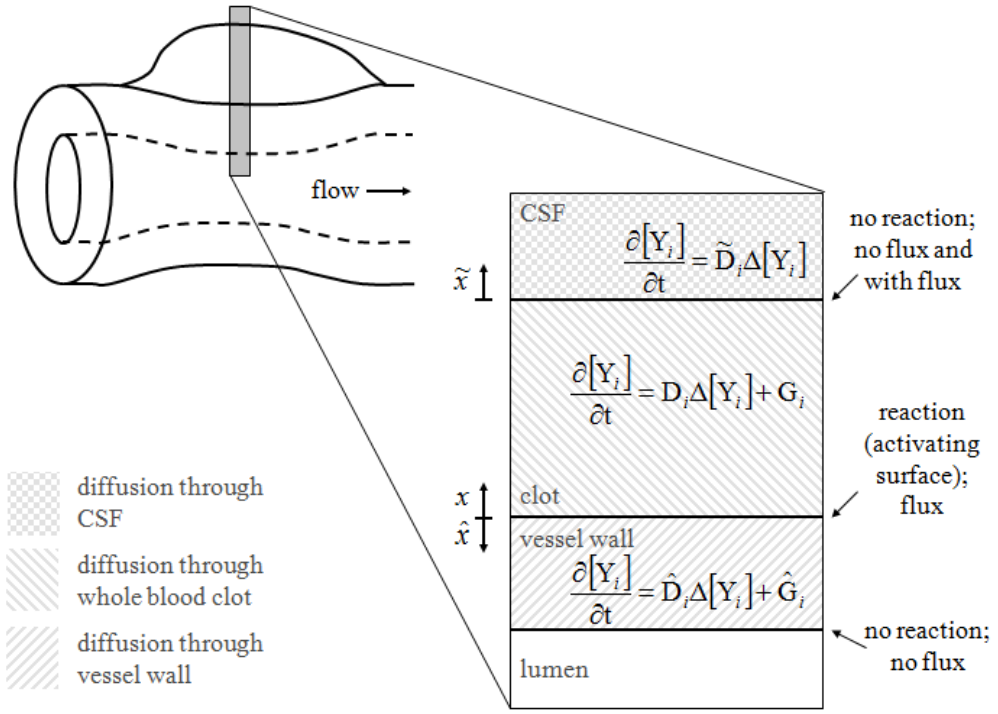

Figure 3
Schema of the proposed model, including reaction and diffusion of clotting factors through the clot. Values at time points at boundaries of the clot provide boundary conditions for the vessel wall and CSF solutions. Each medium requires a different set of diffusivity constants for the factors.

2.1 Existing Model

Anand et al. (2008) introduced a model to describe blood clotting in a quiescent state. This model expands on work previously done by the group to describe clot growth in flowing blood (Anand et al., 2003). Briefly, the more recent model includes 23 reaction-diffusion partial differential equations of the form

$$\frac{\partial[Y_i]}{\partial t} = D\Delta[Y_i] + G_i, i = 1,...,23$$

where i represents each clotting factor of interest. The reaction portion for each factor is provided in equations 1-25.

$$G_{XI} = -\frac{k_{11}[\mathrm{IIa}][\mathrm{XI}]}{K_{11\mathrm{M}} + [\mathrm{XI}]} \tag{1}$$

$$G_{XIa} = \frac{k_{11}[\mathrm{IIa}][\mathrm{XI}]}{K_{11\mathrm{M}} + [\mathrm{XI}]} - h_{11}^{\mathrm{A3}}[\mathrm{XIa}][\mathrm{ATIII}] - h_{11}^{L1}[\mathrm{XIa}][\alpha 1\mathrm{AT}] \tag{2}$$

$$G_{IX} = -\frac{k_{9}[\mathrm{XIa}][\mathrm{IX}]}{K_{9\mathrm{M}} + [\mathrm{IX}]} \tag{3}$$

$$G_{IXa} = \frac{k_{9}[\mathrm{XIa}][\mathrm{IX}]}{K_{9\mathrm{M}} + [\mathrm{IX}]} - h_{9}[\mathrm{IXa}][\mathrm{ATIII}] \tag{4}$$

$$G_{VIII} = -\frac{k_{8}[\mathrm{IIa}][\mathrm{VIII}]}{K_{8\mathrm{M}} + [\mathrm{VIII}]} \tag{5}$$

$$G_{VIIIa} = \frac{k_{8}[\mathrm{IIa}][\mathrm{VIII}]}{K_{8\mathrm{M}} + [\mathrm{VIII}]} - h_{8}[\mathrm{VIIIa}] - \frac{h_{\mathrm{C8}}[\mathrm{APC}][\mathrm{VIIIa}]}{H_{\mathrm{C8M}} + [\mathrm{VIIIa}]} \tag{6}$$

$$G_{X} = -\frac{k_{10}\dfrac{[\mathrm{VIIIa}][\mathrm{IXa}]}{k_{dZ}}[\mathrm{X}]}{K_{10\mathrm{M}}[\mathrm{X}]} \tag{7}$$

$$G_{Xa} = \frac{k_{10}\dfrac{[\mathrm{VIIIa}][\mathrm{IXa}]}{k_{dZ}}[\mathrm{X}]}{K_{10\mathrm{M}}[\mathrm{X}]} - h_{10}[\mathrm{Xa}][\mathrm{ATIII}] - h_{\mathrm{TFPI}}[\mathrm{TFPI}][\mathrm{Xa}] \tag{8}$$

$$G_{\mathrm{V}} = -\frac{k_{5}[\mathrm{IIa}][\mathrm{V}]}{K_{5\mathrm{M}} + [\mathrm{V}]} \tag{9}$$

$$G_{Va} = \frac{k_{5}[\mathrm{IIa}][\mathrm{V}]}{K_{5\mathrm{M}} + [\mathrm{V}]} - h_{5}[\mathrm{Va}] - \frac{h_{\mathrm{C5}}[\mathrm{APC}][\mathrm{Va}]}{H_{\mathrm{C5M}} + [\mathrm{Va}]} \tag{10}$$

$$G_{II} = -\frac{k_2 \frac{[Va][Xa]}{k_{dW}}[II]}{K_{2m} + [II]} \tag{11}$$

$$G_{IIa} = \frac{k_2 \frac{[Va][Xa]}{k_{dW}}[II]}{K_{2m} + [II]} - h_2[IIa][ATIII] \tag{12}$$

$$G_{I} = -\frac{k_1[IIa][I]}{K_{1m} + [I]} \tag{13}$$

$$G_{Ia} = \frac{k_1[IIa][I]}{K_{1m} + [I]} - \frac{h_1[PLA][Ia]}{H_{1m} + [Ia]} \tag{14}$$

$$G_{PLS} = -\frac{k_{PLA}[tPA][PLS]}{K_{PLAM}[PLS]} \tag{15}$$

$$G_{PLA} = \frac{k_{PLA}[tPA][PLS]}{K_{PLAM}[PLS]} - h_{PLA}[PLA][\alpha 2AP] \tag{16}$$

$$G_{tPA} = 0 \tag{17}$$

$$G_{PC} = -\frac{k_{PC}[IIa][PC]}{K_{PCM} + [PC]} \tag{18}$$

$$G_{APC} = \frac{k_{PC}[IIa][PC]}{K_{PCM} + [PC]} - h_{PC}[APC][\alpha 1AT] \tag{19}$$

$$G_{ATIII} = -\left(h_9[IXa] + h_{10}[Xa] + h_2[IIa] + h_{11}^{A3}[XIa]\right)[ATIII] \tag{20}$$

$$G_{TFPI} = -h_{TFPI}[TFPI][Xa] \tag{21}$$

$$G_{\alpha 1AT} = -h_{PC}[APC][\alpha 1AT] - h_{11}^{L1}[XIa][\alpha 1AT] \tag{22}$$

$$G_{\alpha 2AP} = -h_{PLA}[PLA][\alpha 2AP] \tag{23}$$

$$[\mathrm{Z}] = \frac{[\mathrm{VIIIa}][\mathrm{IXa}]}{k_{dZ}} \tag{24}$$

$$[\mathrm{W}] = \frac{[\mathrm{Va}][\mathrm{Xa}]}{k_{dW}} \tag{25}$$

Reaction kinetics, diffusion coefficients, and initial conditions are determined from a literature search, with the results provided in the table in Appendix C, the table on page 18, and Appendix A, respectively. The model is solved using a modified version of a built-in MATLAB function. The pde solver, pdepe, must be altered to allow for a NonNegative requirement, to maintain physically meaningful solutions. Diffusion coefficients determined through the method of Young (Young and Bell, 1980) are provided in the table on page 18.

The model depicts a 2 mm clot (i.e. $0 \leq x \leq L$, where L = 2 mm) over a period of 840 seconds (i.e. $0 \leq t \leq T$, where T = 840 s). A clot is defined as formed when fibrin concentration at any point is greater than or equal to 350 nM. Justification for this concentration is explained in Anand et al. (2008) and is based on the turbidity, or cloudiness, of a clot. The clot is mathematically initiated by setting initial concentrations of active factors to 0.1% the value of their inactive zymogen forms (see the table in Appendix A).

For completeness, we briefly list the boundary conditions of the clot (Anand et al., 2008). The clot is physically initiated by contact with the thrombogenic surface at x = 0 and is mathematically initiated at the boundary by setting the following boundary

conditions given in equations 26 and 27. The values for [TF-VIIa] and an explanation of the development of these boundary conditions are available in Anand et al., 2008.

$$\left.\frac{\partial[\mathrm{IXa}]}{\partial x}\right|_{x=0} = -\frac{k_{7,9}[\mathrm{IX}][\mathrm{TF-VIIa}]}{K_{7,9M}+[\mathrm{IX}]}\frac{L}{D_{IXa}} = -\frac{D_{IX}}{D_{IXa}}\left.\frac{\partial[\mathrm{IX}]}{\partial x}\right|_{x=0} \tag{26}$$

$$\left.\frac{\partial[\mathrm{Xa}]}{\partial x}\right|_{x=0} = -\frac{k_{7,10}[\mathrm{X}][\mathrm{TF-VIIa}]}{K_{7,10M}+[\mathrm{X}]}\frac{L}{D_{Xa}} = -\frac{D_{X}}{D_{Xa}}\left.\frac{\partial[\mathrm{X}]}{\partial x}\right|_{x=0} \tag{27}$$

2.2 Factor XIII

Factor XIIIa (activated plasma transglutaminase) forms γ-glutamyl-ε-lysyl covalent cross-links in mature fibrin (Trumbo and Maurer, 2003). These cross-links increase the mechanical strength of the clot as well as the resistance to the degradatory effects of plasmin by binding α2-antiplasmin to the fibrin scaffold (Lewis et al., 1997; Nielsen, 2006(c)). Factor XIII is produced in zymogen form with A and B subunits by macrophages, megakaryocytes, and the liver (Lewis et al., 1997; Lehrer and Ganz, 2001) and circulates both in plasma and platelets. Platelets lyse during the clotting process, releasing stores of factor XIII, which is quickly activated to form factor XIIIa by the removal of the inactive B subunit and exposure of the active site on the A subunit (Ariens et al., 2000; Lehrer and Ganz, 2001; Greenberg et al., 2001).

Bakker et al. (2005) implicate tissue-type transglutaminase in small artery remodeling by its ability to “modify matrix proteins”. They cultured vessels in vitro at low pressures to chronically set inner radius low. “However, they have no intrinsic tendency to remodel at this pressure” (Bakker et al., 2005). The zymogen for tissue-type

transglutaminase (tTG) is composed of two of the A subunits, which are cleaved to provide available active sites on each subunit. The activation of factor XIII to factor XIIIa follows Michaelis-Menten kinetics (equations 28 and 29). The formation of non-soluble cross-linked fibrin (IaC) can then be described by equation 30. Equation 30 includes a constant, C, which accounts for plasmic degradation of cross-linked fibrin being significantly slower than that of factor Ia. An appropriate value for this parameter is 0.68 (Francis and Marder, 1988). The appropriate kinetic parameters for equations 28-30 are provided in Table 2.

$$G_{XIII} = -\frac{k_{13}[\mathrm{IIa}][\mathrm{XIII}]}{K_{13\mathrm{M}} + [\mathrm{XIII}]} \tag{28}$$

$$G_{XIIIa} = \frac{k_{13}[\mathrm{IIa}][\mathrm{XIII}]}{K_{13\mathrm{M}} + [\mathrm{XIII}]} - \frac{h_{13}[\mathrm{Ia}][\mathrm{XIIIa}]}{H_{13\mathrm{M}} + [\mathrm{XIIIa}]} \tag{29}$$

$$G_{IaC} = \frac{h_{13}[\mathrm{Ia}][\mathrm{XIIIa}]}{H_{13\mathrm{M}} + [\mathrm{XIIIa}]} - C\frac{h_{1}[\mathrm{PLA}][\mathrm{Ia}]}{H_{1m} + [\mathrm{Ia}]} \tag{30}$$

Table 2
Kinetic parameters for factor XIII and cross-linked fibrin. The activation of factor XIII and the cross-linking of fibrin follow Michaelis-Menten kinetics with kinetic parameters shown below.

kinetic parameter	reaction	value	source
k_{13}	XIII → XIIIa	508000 nM	Trumbo and Maurer, 2003
K_{13M}	XIII → XIIIa	384 min^{-1}	Trumbo and Maurer, 2003
k_{1ac}	Ia → cross-linked fibrin	6200 nM	Lewis et al., 1997
K_{1acM}	Ia → cross-linked fibrin	1872 min^{-1}	Lewis et al., 1997

Additionally, equation 14 is modified to reflect the primary loss of activated fibrin due to its cross-linking by factor XIIIa rather than its degradation by plasmin (see equation 31).

$$G_{Ia} = \frac{k_1[\mathrm{IIa}][\mathrm{I}]}{K_{1m} + [\mathrm{I}]} - \frac{h_1[\mathrm{PLA}][\mathrm{Ia}]}{H_{1m} + [\mathrm{Ia}]} \tag{31}$$

2.3 Diffusion through Clot

In the Anand model diffusion coefficients of clotting factors through the clot are calculated using the method put forth by Young (Young and Bell, 1980). The factors were treated as diffusing through a homogeneous medium. However, diffusion coefficients vary with position and time as the clot began to form and fibrin fibrils impede the diffusion of molecules. Additionally, the effect of red blood cells in a whole blood clot was not considered. These simplifications yield acceptable results (Anand et al., 2008), so we carry them through in the current work. Diffusion coefficients in the clot are given in the table on page 19.

2.4 Diffusion through Arterial Wall

Describing the transport of molecules through an artery wall is of interest in two particular fields: drug delivery (Goriely et al., 2007; Hwang and Edelman, 2002; Levin et al., 2004) and the diffusion of growth factors into an artery during plaque development in atherosclerosis (Dabagh et al., 2007; Fry, 1985; Kim, 1996; Saidel,

1987; Tarbell, 2003). The transport of molecules through the arterial wall is dependent on the wall structure, which varies significantly between arterial beds (e.g. cerebral vs. systemic) (Hwang, 2002).

In order to understand the progression of cerebral vasospasm we must understand the time course and magnitude of the exposure of arterial wall components to vasoactive compounds liberated by the clot, neural cells, and inflammatory response. Molecules are introduced into the wall from the adventitial side, driven by a concentration gradient and moving against the transmural pressure gradient. Total flux includes the diffusive flux and the convective flux (Fry, 1985). In cerebral vasospasm the vessel is constricted, increasing flow and decreasing pressure. We will neglect the pressure gradient resulting from the blood pressure inside the artery, simplifying the flux to the diffusion term only.

The wall of an artery is split into three layers (Figure 4). The inner most layer of the constricted artery, the intima, is composed of a single leaky layer of endothelial cells. The middle layer, or media, is composed of smooth muscle cells, collagen, elastic fibers, and proteoglycans, which sequester water. The outermost layer, or adventitia, primarily composed primarily of type I collagen, and fibroblasts. The proportion of contents in an artery vary by location and function, however cerebral arteries are classified as muscular arteries which have a high diffusive resistance in the media (Fry, 1985; Hwang and Edelman, 2002).

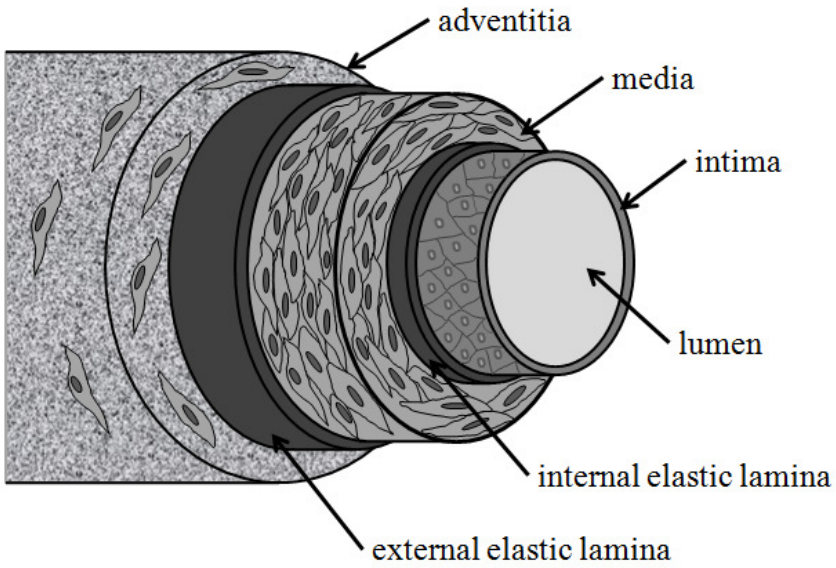

Figure 4
Typical arterial wall structure.

The internal elastic lamina, which separates the endothelium from the media, acts as a physical barrier and reaction site for drugs delivered into the lumen of the artery (Goriely, 2007; Creel, 2000). Diffusion across this layer must take into account the area of the tissue taken up by pores (Goriely, 2007). This layer of tissue must be accounted for in describing diffusion of medicine from the lumen into the artery. However, our primary interest is the interaction of the vasoactive species with smooth muscle cells, which will be reached before the internal elastic lamellae.

Many groups have pursued modeling diffusion across an arterial wall (Goriely, 2007; Dabagh, 2007; Fry, 1985; Hwang and Edelman, 2002; Kim et al., 1996; Feenstra and Taylor, 2009). The effective diffusivity of drugs when applied to the perivascular

side are approximately half that of drugs applied to the endovascular side of the artery due to the convective effects of transmural pressure (Creel et al., 2000).

When all complexities are included each layer of the wall must be accounted for separately (Fry, 1985). The endothelium allows transport through endothelial cells and pores between cells. In the internal elastic lamina, transport occurs through the sheet and through pores in the sheet. Adventitial and medial layers allow transport between cells and matrix.

As Hwang and Edelman suggest, "because the heterogeneity of the arterial wall is highly regular…it is convenient to use a lumped effective diffusivity parameter to characterize bulk drug transport properties in the arterial wall" (Hwang and Edelman, 2002). We treat the arterial wall as a homogeneous continuum composed of a porous medium. We neglect the effects of the adventitia and endothelium, calculating effective diffusion coefficients through the wall as a function of the void fraction (i.e. the space that is not cells and is therefore available for diffusion) of the media. "The adventitia itself is a relatively diffuse structure and seems unlikely to present a major barrier" (Goriely et al., 2007). For example, the effective diffusivity of heparin in media and intima have been shown to be the same and increased in the adventitia (Lovich and Edelman, 1999). However, Goriely et al. note that there is an external elastic lamina between the adventitia and the media, which would affect diffusivity in a typical artery. However, we neglect this barrier, since an external elastic lamina does not exist in cerebral arteries.

We use the method of Weissberg to determine the effective diffusivity through the arterial wall (Weissberg, 1963). The void fraction of the arterial wall is 0.75 (Murata, 1985) and the viscosity of water is 0.69 cP. The effective diffusion coefficient of each species is given in the table on page 19.

We assume constant diffusion coefficient as a function of time and space. However, as cerebral vasospasm progresses, the structure of the wall would also change as the orientation of cells and matrix structures change (Hwang and Edelman, 2002).

The basilar artery, a major artery which supplies the brain with blood, is often used in studies of cerebral vasospasm. Typical adult human basilar arterial wall thickness is approximately 250 μm, which provides a generic value for the diffusion distance, $\hat{L}$, through the artery wall (Pico et al., 2006). Further discussion of this value is provided in Future Work.

2.5 Diffusion through CSF

Diffusion coefficients of the clotting factors in the CSF are calculated, once again, using the Young method and are given in Table 3 (Young and Bell, 1980).

Table 3
Diffusion coefficients of clotting species in plasma and CSF and effective diffusion coefficients in wall.

species	molecular mass (Da)	diffusion coefficient in plasma (cm^2/s)	diffusion coefficient in water (cm^2/s)	effective diffusion coefficient in wall (cm^2/s)	diffusion coefficient in CSF (cm^2/s)
fibrinogen (I)	340000	3.1×10^{-7}	5.37×10^{-7}	3.52×10^{-7}	4.36×10^{-7}
fibrin (Ia)	660000	2.47×10^{-7}	4.31×10^{-7}	2.82×10^{-7}	3.50×10^{-7}
prothrombin (II)	72000	5.21×10^{-7}	9.01×10^{-7}	5.91×10^{-7}	7.31×10^{-7}
thrombin (IIa)	37000	6.47×10^{-7}	1.13×10^{-6}	7.38×10^{-7}	9.13×10^{-7}
V	330000	3.12×10^{-7}	5.42×10^{-7}	3.56×10^{-7}	4.40×10^{-7}
Va	179000	3.82×10^{-7}	6.65×10^{-7}	4.36×10^{-7}	5.40×10^{-7}
VIII	330000	3.12×10^{-7}	5.42×10^{-7}	3.56×10^{-7}	4.40×10^{-7}
VIIIa	166000	3.92×10^{-7}	6.82×10^{-7}	4.47×10^{-7}	5.54×10^{-7}
IX	56000	5.63×10^{-7}	9.80×10^{-7}	6.42×10^{-7}	7.95×10^{-7}
IXa	41000	6.25×10^{-7}	1.09×10^{-6}	7.13×10^{-7}	8.83×10^{-7}
X	56000	5.63×10^{-7}	9.80×10^{-7}	6.42×10^{-7}	7.95×10^{-7}
Xa	25000	7.37×10^{-7}	1.28×10^{-6}	8.41×10^{-7}	1.04×10^{-6}
XI	160000	3.97×10^{-7}	6.91×10^{-7}	4.53×10^{-7}	5.61×10^{-7}
Xia	80000	5.0×10^{-7}	8.70×10^{-7}	5.70×10^{-7}	7.06×10^{-7}
XIII	320000	3.15×10^{-7}	5.48×10^{-7}	3.59×10^{-7}	4.45×10^{-7}
XIIIa	166000	3.92×10^{-7}	6.82×10^{-7}	4.47×10^{-7}	5.54×10^{-7}
a1AT	51000	5.82×10^{-7}	1.01×10^{-6}	6.63×10^{-7}	8.21×10^{-7}
tPA	68000	5.28×10^{-7}	9.18×10^{-7}	6.02×10^{-7}	7.46×10^{-7}
plasminogen	92000	4.81×10^{-7}	8.30×10^{-7}	5.44×10^{-7}	6.74×10^{-7}
plasmin	85000	4.93×10^{-7}	8.53×10^{-7}	5.59×10^{-7}	6.92×10^{-7}
a2AP	70000	5.25×10^{-7}	9.10×10^{-7}	5.96×10^{-7}	7.38×10^{-7}
PC	62000	5.44×10^{-7}	9.47×10^{-7}	6.21×10^{-7}	7.69×10^{-7}
APC	60000	5.50×10^{-7}	9.58×10^{-7}	6.28×10^{-7}	7.77×10^{-7}
ATIII	58000	5.57×10^{-7}	9.68×10^{-7}	6.35×10^{-7}	7.86×10^{-7}
TFPI	40000	6.30×10^{-7}	1.10×10^{-6}	7.19×10^{-7}	8.90×10^{-7}

2.6 Flux between Domains

The flux between each domain forms a unique set of boundary conditions for each domain (Figure 5).

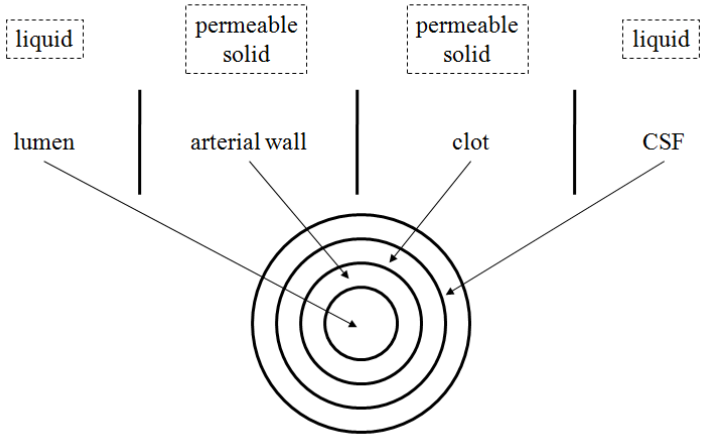

Figure 5
Schema of the boundary conditions that exist at the interface between each domain.

Flux of clotting factors from the clot to the arterial wall occur over a permeable solid-permeable solid interface (Truskey et al., 2004), which can be described by

$$\frac{\partial C_i}{\partial t} = k\Phi_i\left(C_i\Big|_{\text{clot}} - C_i\Big|_{\text{wall}}\right) \tag{32}$$

where C_i is the concentration of each species at the boundary, and k is the permeability coefficient, defined as

$$k = \frac{D_{eff}\Phi}{L} \tag{33}$$

The partition coefficient, Φ, is defined as

$$\Phi = \frac{kAV}{\varepsilon} \tag{34}$$

where

$$k_{AV} = \frac{\text{available volume}}{\text{total volume}} \tag{35}$$

and

$$\varepsilon = \frac{\text{void volume}}{\text{total volume}}$$

Therefore,

$$\Phi = \frac{\frac{\text{available volume}}{\text{total volume}}}{\frac{\text{void volume}}{\text{total volume}}} = \frac{\text{available volume}}{\text{void volume}} \tag{36}$$

Void volume is defined as the volume of the permeable solid that is vacant of solid material and able to contain diffusing substances. Available volume is defined as the volume of the permeable solid that is accessible from other gaps. We select the conservative estimate of Φ, as the material with the lower value would potentially act as a limiting factor in the rate of diffusion.

Similarly, flux from the clot into the CSF can be described as occurring at a permeable solid-liquid interface (Truskey et al, 2004). Therefore,

$$\frac{\partial C_i}{\partial t} = k\left(\Phi_i C_i \Big|_{\text{clot}} - C_i \Big|_{\text{CSF}} \right). \tag{37}$$

We neglect any transfer that occurs between the lumen of the artery and the arterial wall, although this could also be described with the permeable solid-liquid interface form.

2.7 Reaction with Wall Components

As each species diffuses into the arterial wall, reactions occur with the extracellular matrix and cells (e.g. fibroblasts, smooth muscle cells, endothelial cells), impeding the flux through the wall. Thrombin, a smooth muscle cell mitogen, is used here to illustrate the reaction of one of the species with wall components. The general form for the reaction component, G, for thrombin in the artery wall is given below.

$$G_{IIa} = -\frac{k_d [\text{SMC reaction sites}][\text{IIa}]}{K_{11\text{M}} + [\text{IIa}]} \tag{38}$$

where $[\text{SMC reaction sites}] = [\text{SMC}]\left(\frac{\text{reaction sites}}{\text{SMC}}\right)$

Dabagh et al.(2007) estimate the volume fraction of smooth muscle cells, [SMC], to be 0.4 – 0.7. Additional experiments would have to be performed to confirm that Michaelis-Menten kinetics are appropriate for this reaction and to determine the kinetic constants, k_d and K_{11M}.

3. STRUCTURE OF PROGRAM

Each domain (i.e. the clot, arterial wall, and CSF) is solved using separate code. Each domain is defined by its boundary conditions, initial conditions, and reaction-diffusion equations, which are then solved by a modified pdepe code. Each domain yields a program flow as shown in Figure 6. Figure 7 shows a schematic of the entire program, illustrating the output of the clot domain providing boundary conditions for the CSF and vessel wall domains. The required form for each domain is provided in the tables in Appendix B.

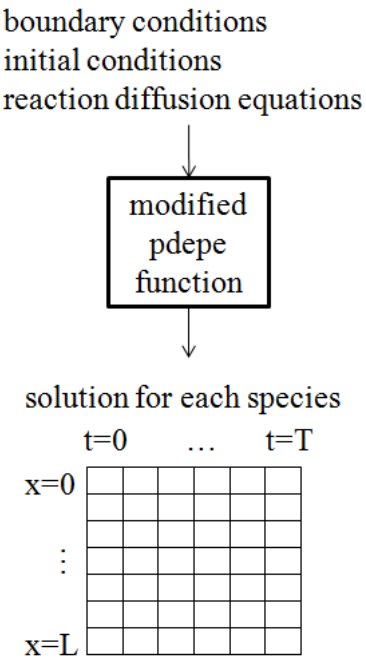

Figure 6
Flow of program for each domain.

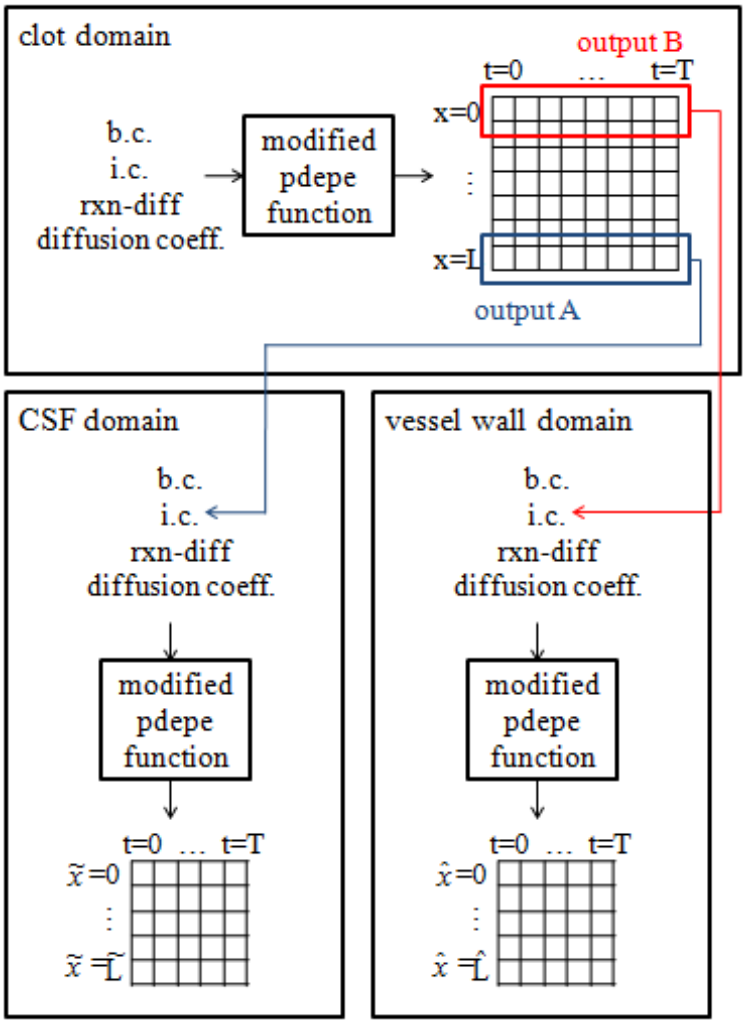

Figure 7
Schema of flow of entire model. Includes the feed of solutions from the clot domain into the initial conditions for the CSF and vessel wall domains.

4. RESULTS OF SIMPLIFIED APPROACH

Although this system of partial differential equations captures many interesting and important details about the clotting process in subarachnoid hemorrhage and can be used to describe numerous pathological conditions (see Anand et al., 2003 and Anand et. al, 2008), we can greatly simplify the kinetics by describing these reactions with first order reactions representing lumped parameter models. This essentially is allowed by assuming that an excess quantity of the substrate and the enzyme are present so that there is no rate limiting reactant.

Two particular subgroups of the cascade emerge as central for the cerebral vasospasm problem. First, the rate at which the clot is degraded by plasmin is important for understanding the exposure of the adjacent artery to clot factors (see Figure 8). Second, the formation of the clot, with particular emphasis on the crosslinking of fibrin by transglutaminase (factor XIIIa) provides the time course for the clot becoming insoluble (see figure on page 30).

4.1 Degradation of Cross-linked Fibrin

For the first reaction of interest (Figure 8) we perform nonlinear regression. The data given in Figure 9 are reproduced from Figure 3 of Wootton et al., 2001. We focus on the experimental results at low shear rates (4 dyn/cm^2) to best represent the stagnant blood following subarachnoid hemorrhage.

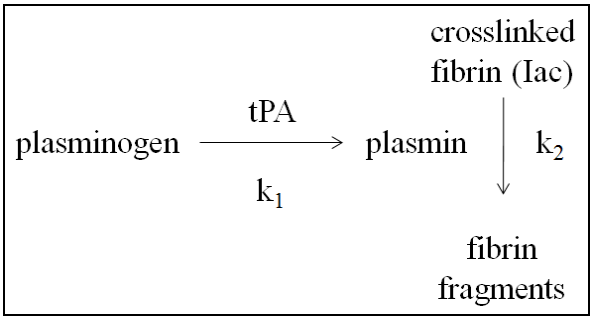

Figure 8
Schema of reaction which yields fibrin fragments through degradation of fibrin by plasmin.

Assuming first-rate kinetics, these reactions are described mathematically as,

$$\frac{d[\text{pla}]}{dt} = k_1[\text{tPA}][\text{pls}]$$

$$\int_0^s \frac{d[\text{pla}]}{dt}\,dt = \int_0^s k_1[\text{tPA}][\text{pls}]dt$$

$$[\text{pla}]\Big|_s = k_1[\text{tPA}]\int_0^s [\text{pls}]dt \tag{39}$$

and

$$\frac{d[\text{FDP}]}{dt} = k_2[\text{Iac}][\text{pla}]$$

$$\int_0^s \frac{d[\text{FDP}]}{dt}\,dt = \int_0^s k_2[\text{Iac}][\text{pla}]dt$$

$$[\text{FDP}]\Big|_s = k_2[\text{Iac}]\int_0^s [\text{pla}]dt \tag{40}$$

With substitution,

$$[\text{FDP}]\big|_s = k_2 k_1 [\text{Iac}][\text{tPA}] \int_0^s \int_0^s [\text{pls}] dt dt$$

$$\left.\frac{d[\text{FDP}]}{dt}\right|_s = k_2 k_1 [\text{Iac}][\text{tPA}] \int_0^s [\text{pls}] dt$$

$$\left.\frac{d^2[\text{FDP}]}{dt^2}\right|_s = k_2 k_1 [\text{Iac}][\text{tPA}][\text{pls}] \tag{41}$$

The loss of fibrin through degradation by plasmin assumes a sigmoidal shape experimentally (Figure 9) (Wootton et al., 2001), which takes the form

$$[\text{FDP}] = \frac{a}{b + g\mathrm{e}^{-h\mathrm{t}+k}} + m \tag{42}$$

Using the Matlab built-in function lsqcurvefit, which employs the Levenberg-Marquardt algorithm, we solve for the values of each parameter to determine an equation to describe the degradation of fibrin (Iac) (Appendix D). Results of the fit are given in Figure 9.

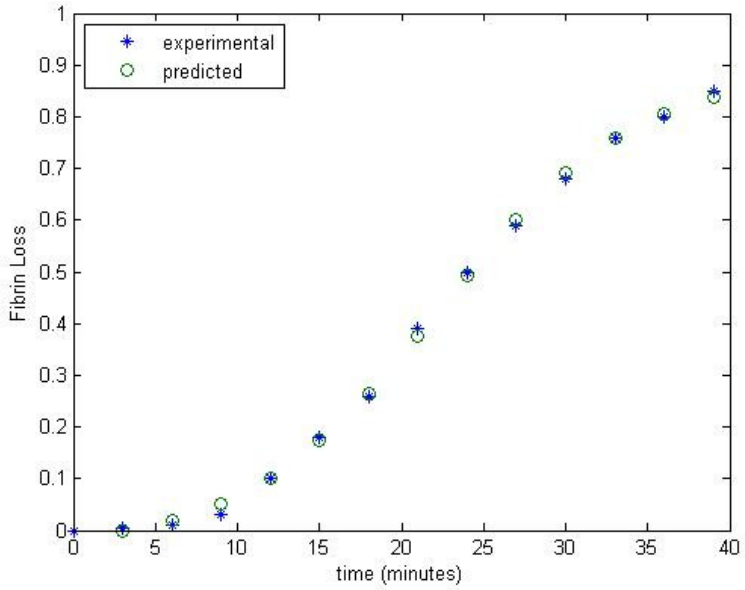

Figure 9
Fibrin loss due to degradation by plasmin. Experimental (*) results reproduced from Wootton et al., 2001, Figure 3. Predicted values (°) determined from nonlinear regression.

Results of nonlinear regression yield

a = 0.0184
b = 0.0198
g = 1.9018
h = 0.1679
k = 4.8323
m = -0.0368

with a norm of residuals of 0.0017, or

$$[\mathrm{FDP}] = \frac{0.0184}{0.0198 + 1.9018 e^{-0.1679t + 4.8323}} - 0.0368 \tag{43}$$

and, therefore,

$$\frac{d^2[\mathrm{FDP}]}{dt^2} = 0.0037570\frac{\left(e^{-0.16788t+4.8323}\right)^2}{\left(0.019847+1.9018e^{-0.16788t+4.8323}\right)^3} - 0.00098776\frac{\left(e^{-0.16788t+4.8323}\right)^2}{\left(0.019847+1.9018e^{-0.16788t+4.8323}\right)^2} = k_2k_1[\mathrm{Iac}][\mathrm{tPA}][\mathrm{pls}] \quad (44)$$

Therefore,

$$k_2k_1 = \frac{0.0037570\dfrac{\left(e^{-0.16788t+4.8323}\right)^2}{\left(0.019847+1.9018e^{-0.16788t+4.8323}\right)^3}}{[\mathrm{Iac}][\mathrm{tPA}][\mathrm{pls}]} - \frac{0.00098776\dfrac{\left(e^{-0.16788t+4.8323}\right)^2}{\left(0.019847+1.9018e^{-0.16788t+4.8323}\right)^2}}{[\mathrm{Iac}][\mathrm{tPA}][\mathrm{pls}]} \quad (45)$$

We assume that plasminogen (pls) and tPA are not consumed in the reaction and are available in sufficient quantities to prevent any rate-limiting effects. Therefore, [pls] = $[\mathrm{pls}]_o$ and [tPA]=$[\mathrm{tPA}]_o$. If we were to consider the behavior over long periods we would have to account for the half-lives of each molecule, but we neglect that complication here.

tPA is injected at an initial concentration of 6.94 μM (0.5 μg/ml). The initial plasminogen would be based on the PPP (platelet-poor plasma) sample. Since we neglect the more complicated requirements of a solution where feedback is considered, [Iac] is also treated as a constant value, which is determined by the experimental conditions. Wootton et al. did not report this value, but the experiment could be repeated to confirm

the value. In this case we are unable to separate the values of k_1 and k_2, as more experiments would be required. However, this lumped sum parameter solution is sufficient for continuum mixture models.

4.2 Formation of Cross-linked Fibrin

The second set of reactions of interest (Figure 10) are described following a similar process as given above.

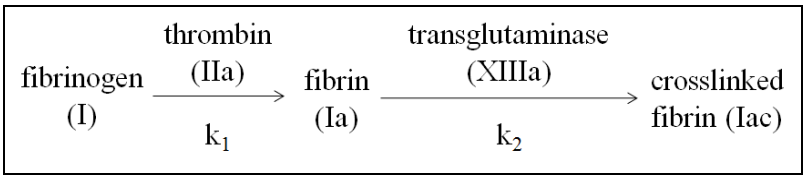

Figure 10
Schema of fibrinogen being converted through two reactions to cross-linked fibrin.

$$\frac{d[\mathrm{Ia}]}{dt} = k_1[\mathrm{I}][\mathrm{IIa}]$$

$$\int_0^s \frac{d[\mathrm{Ia}]}{dt}\,dt = \int_0^s k_1[\mathrm{I}][\mathrm{IIa}]dt$$

$$[\mathrm{Ia}]\big|_s = k_1[\mathrm{IIa}]\int_0^s [\mathrm{I}]dt \tag{46}$$

Similarly,

$$\frac{d[\text{Iac}]}{dt} = k_2[\text{Ia}][\text{XIIIa}]$$

$$\int_0^s \frac{d[\text{Iac}]}{dt} dt = \int_0^s k_2[\text{Ia}][\text{XIIIa}] dt$$

$$[\text{Iac}]\big|_s = k_2[\text{XIIIa}]\int_0^s [\text{Ia}] dt \tag{47}$$

where we similarly assume that $[\text{XIIIa}] = [\text{XIIIa}]_0$ and $[\text{IIa}] = [\text{IIa}]_0$.

In contrast to the degradation reactions, the solution to these staggered reactions may be solved in two steps, in order to define k_1 and k_2 independently. Weisel et al. (1992) provide a solution to describe the formation of fibrin (I) beginning from the conversion from fibrin. This solution yields a sigmoidal shape (Figure 11) which is most appropriately modeled as

$$[\text{Ia}] = a + b\text{e}^{ct^d} \tag{48}$$

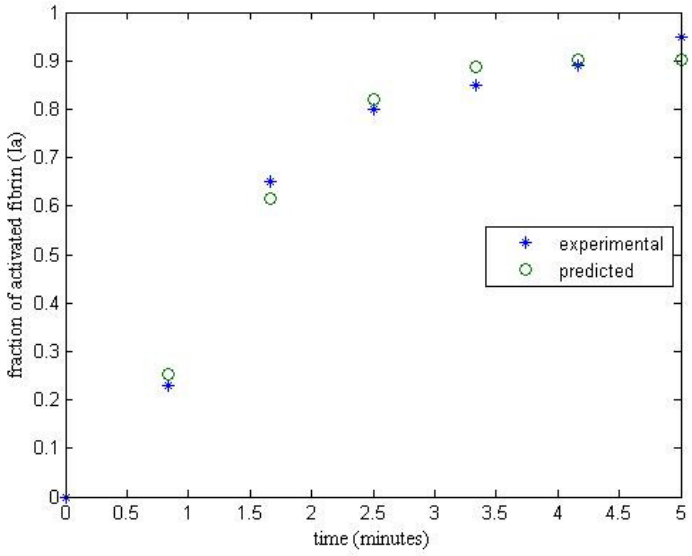

Figure 11
Fraction of activated fibrin formed in the presence of thrombin (factor IIa). Experimental (*) results reproduced from Weisel and Nagaswami, 1992, Figure 2. Predicted values (^{o}) determined from nonlinear regression.

Results of the nonlinear regression yield

a = 0.9036
b = -0.9111
c = -0.4642
d = 1.7811

with a norm of residuals of 0.0057, or

$$[\mathrm{Ia}] = 0.9036 - 0.9111\mathrm{e}^{-0.4642\mathrm{t}^{1.7811}} \tag{49}$$

Therefore,

$$\frac{d[\mathrm{Ia}]}{dt} = 0.7533\mathrm{t}^{0.7811\mathrm{t}}\mathrm{e}^{-0.4642\mathrm{t}^{1.7811}} \tag{50}$$

and, from equations 45 and 49,

$$k_1 = \frac{0.7533\mathrm{t}^{0.7811\mathrm{t}}\mathrm{e}^{-0.4642\mathrm{t}^{1.7811}}}{[\mathrm{IIa}][\mathrm{I}]} \tag{51}$$

where [IIa] is about 1 NIH unit/mL and [I] = 0.5-1.5 mg/ml (Weisel, 1992). Additional experiments should be performed to narrow possible initial values.

The formation of the final product, Iac, assumes a sigmoidal shape experimentally (Figure 12) (Siebenlist et al., 2001), which also takes the form

$$[\mathrm{Iac}] = a + b\mathrm{e}^{c\mathrm{t}^d} \tag{52}$$

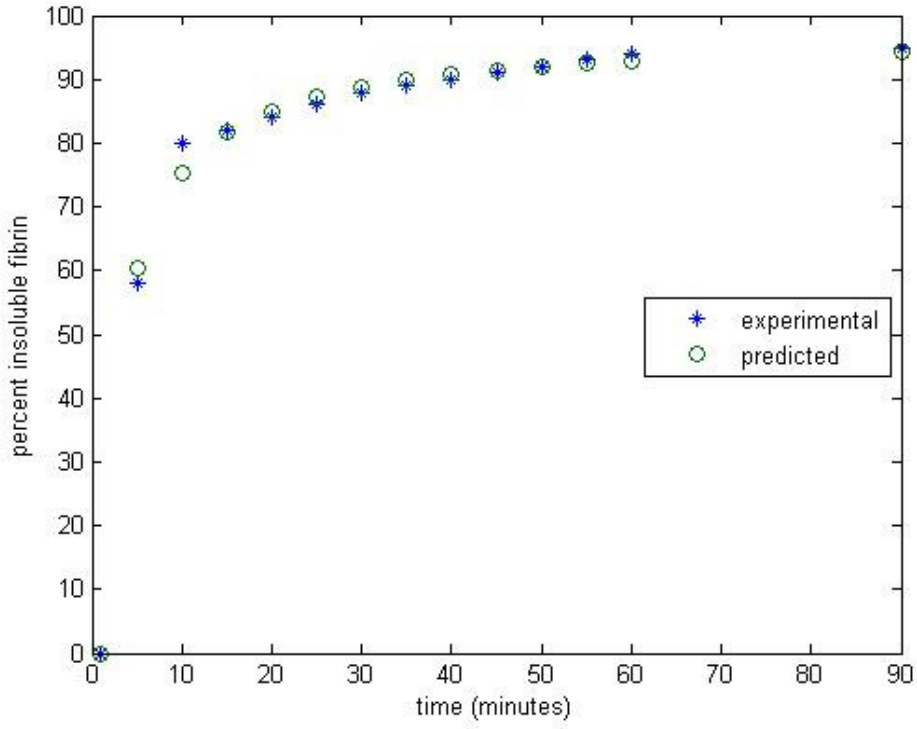

Figure 12
Percent insoluble fibrin formed in the presence of transglutaminase (factor XIIIa). Experimental (*) results reproduced from Siebenlist et al., 2001, Figure 4. Predicted values (°) determined from nonlinear regression.

The nonlinear regression yields

a = 96.1
b = -1066.2
c = -2.404
d = 0.2140

with a norm of residuals of 34.8750, or

$$[\mathrm{Iac}] = 96.1 - 1066.2\mathrm{e}^{-2.404\mathrm{t}^{0.214}} \tag{53}$$

Therefore,

$$\frac{d[\mathrm{Iac}]}{dt} = 548.8\mathrm{t}^{-0.7860\mathrm{t}}\mathrm{e}^{-2.404\mathrm{t}^{0.2140}} \tag{54}$$

and, from equations 46 and 53,

$$k_2 = \frac{548.8\mathrm{t}^{-0.7860\mathrm{t}}\mathrm{e}^{-2.404\mathrm{t}^{0.2140}}}{[\mathrm{XIIIa}][\mathrm{Ia}]} \tag{55}$$

where [XIIIa] = 100 Loewy u/ml and [Ia] is provided by the solution in equation 48 (Siebenlist, 2001).

5. FUTURE WORK

Simplifying assumptions are made in the proposed model to allow for computational ease. Here we provide a list of future complexities that may be added to the model.

As noted in the table on page 2, multiple molecules have been implicated as primary in the progression of cerebral vasospasm. The proposed model focuses on members of the clotting cascade. Future models should be extended to include additional molecules that are released by blood components, neural tissue, and the imflammatory process, such as PDFG-AB, Endothelin-1, TGF-β, bilirubin oxidation products, and nitric oxide. Molecules with the strongest tissue response for vasoconstriction, vasodilation, and smooth muscle cell proliferation are of particular importance.

The proposed model treats the arterial wall as a homogeneous medium composed of smooth muscle cells and water. As discussed previously, the composition of the arterial wall varies with depth and includes additional cells (e.g. endothelial cells and fibroblasts) and structural components (e.g. types I, III, and IV collagen and elastic fibers). Each structure and cell interacts uniquely with each molecule of interest, acting as potentially both physical barriers and reaction sites.

Diffusion rates would also vary through each layer, depending on the density of cells and structural components. Including blood pressure would resist the diffusion of products from the adventitial to endothelial surfaces.

As cerebral vasospasm progresses the geometry of the wall changes, affecting the travel distance of each species. Additionally, smooth muscle cell proliferation increases

smooth muscle cell density, resulting in an increasing consumption of molecules of interest.

The supply and loss of each clotting factor is dependent on the complex channel system within a whole blood clot (Adolph et al., 1997). These networks of caniculi, as described by Adolph et al., in particular affect the rate of fibrinolysis of the clot, based on supply of tPA and uPA to the interior of the clot. Additionally, although the CSF is treated essentially as a sink for all clotting factors at the outer edge of the clot, the constant flow of CSF would increase the rate at which factors are flushed from the area, increasing the concentration gradient across the barrier and, by extension, an increased loss of all species.

As mentioned previously, initial clot volume is a factor in predicting the clinical outcome of an SAH patient. Altering the thickness of the clot (i.e. the L value in the clot domain) and the thickness of the artery wall (i.e. the $\hat{L}$ value in the artery wall domain) provides patient specific predictions of concentrations within the artery wall.

Improvements can be made in the proposed simplified models by repeating the reported experiments to confirm precise concentrations of each reactant used. Additional experiments could be used to confirm the robustness of the model.

6. CONCLUSION

Cerebral vasospasm following subarachnoid hemorrhage is a leading cause of morbidity and mortality following patient survival of the initial bleed. Using mathematical modeling to predict the concentration of vasoactive molecules through the time course of vasospasm will provide the insight to determine which molecules are of primary importance in the progression of the condition, allowing clinicians to treat subarachnoid hemorrhage patients by addressing the root cause.

Here we develop the theoretical framework for a mathematical model to describe the diffusion of vasoactive substances from a clot into the arterial wall following subarachnoid hemorrhage. The initial approach, containing a system of 26 PDEs, is a comprehensive and complicated method for describing the clot kinetics involved in the progression of cerebral vasospasm. However, with simplified kinetics and a focus on fewer equations we are able to elucidate sufficient parameters for a continuum mixture model in the initial stages of clotting following subarachnoid hemorrhage.

REFERENCES

Adolph, R., Vorp, D., Steed, D., Webster, M., Kameneva, M., Watkins, S., 1997. Cellular content and permeability of intraluminal thrombus in abdominal aortic aneurysm. J. Vasc. Surg. 25, 916-926.

Anand, M., Rajagopal, K., Rajagopal, K., 2003. A model incorporating some of the mechanical and biochemical factors underlying clot formation and dissolution in flowing blood. J.Theor. Med. 5 (3-4), 183-218.

Anand, M., Rajagopal, K., Rajagopal, K.R., 2008. A model for the formation, growth, and lysis of clots in quiescent plasma. A comparison between the effects of antithrombin III deficiency and protein C deficiency. J. Theor. Biol. 253 (4), 725-738.

Ariens, R., Philippou, Nagaswami, C., Weisel, J., Lane, D., Grant, P., 2000. The factor XIII V34L polymorphism accelerates thrombin activation of factor XIII and affects cross-linked fibrin structure. Hem. Thromb. Vasc. Biol. 96 (3), 988-995.

Ataullakhanov, F., Zarnitsina, V., Pokhilko, A., Lobanov, A., Morozova, O., 2002. Spatio-temporal dynamics of blood coagulation and pattern formation, a theoretical approach. Int. J. Bifurc.Chaos. 12 (9), 1985-2002.

Bakker, E., Buus, C., Spaan, J., Perree, J., Ganga, A., Rolf, T., Sorop, O., Bramsen, L., Mulvany, M., VanBavel, E., 2005. Small artery remodeling depends on tissue-type transglutaminase. Circ. Res. 96, 119-126.

Bakker, E., Pistea, A., Spaan, J., Rolf, T., de Vries, C., Rooijen, N., Candi, E., VanBavel, E., 2006. Flow-dependent remodeling of small arteries in mice deficient for tissue-type transglutaminase: possible compensation for macrophage-derived factor XIII. Circ. Res. 99, 86-92.

Baldwin, S., Basmadjian, D., 1994. A mathematical model of thrombin production in blood coagulation, part I: the sparsely covered membrane case. Ann. Biomed. Eng. 22, 357-370.

Bar-Shavit, R., Benezra, M., Eldor, A., Hy-Am, E., Fenton, J., Wilner, G., Vlodavsky, I., 1990. Thrombin immobilized to extracellular matrix is a potent mitogen for vascular smooth muscle cells: nonenzymatic mode of action. Cell Reg. 1, 453-463.

Blomback, B., 1996. Fibrinogen and fibrin – proteins with complex roles in hemostasis and thrombosis. Thromb.Res. 83 (1), 1-75.

Bloomfield, I., 1998. Effects of proteins, blood cells and glucose on the viscosity of cerebrospinal fluid. Ped. Neurosurg. 28 (5), 246-251.

Clark, J., Sharp, F., 2006. Bilirubin oxidation products (BOXes) and their role in cerebral vasospasm after subarachnoid hemorrhage. J. of Cer. Blood Flow & Met. 26, 1223-1233.

Creel, C., Lovich, M., Edelman, E., 2000. Arterial paclitaxel distribution and deposition. Circ. Res. 86, 879-884.

Dabagh, M., Jalali, P., Tynjala, T., Sarkomaa, P., 2007. Molecular transport in the arterial wall with variation of shape and configuration of smooth muscle cells. IFMBE Proc. 14 (1), 41-45.

Fassbender, K., Hodapp, B, Rossol, S., Bertsch, T., Schmeck, J., Schutt, S., Fritzinger, M., Horn, P., Vajkoczy, Wendel-Wellner, M., Ragoschke, A., Kuehl, S., Brunner, J., Schurer, L, Schmiedeck, P., Hennerici, M., 2000. Endothelin-1 in subarachnoid hemorrhage: an acute-phase reactant produced by cerebrospinal fluid leukocytes. Stroke. 31, 2971-2975.

Feenstra, P.H., Taylor, C.A., 2009. Transport in artery walls: a sequential porohyperelastic-transport approach. Comput Meth Biomech Biomed Eng. 12, 263-276.

Flood, C., Akinwunmi, J., Lagord, C., Caniel, M., Berry, M., Jackowski, A., Logan, A., 2001. Patients with subarachnoid hemorrhage: titers derived from exogenous and endogenous sources. J. Cerebral Blood Flow and Metabolism. 21, 157-162.

Francis, C., Marder, V., 1988. Increased resistance to plasmic degradation of fibrin with highly crosslinked α-polymer chains formed at high factor XIII concentrations. Blood. 71 (5), 1361-1365.

Fry, D., 1985. Steady-state macromolecular transport across a multilayered arterial wall. Math. Model. 6, 353-368.

Furie, B., Furie, B.C., 2000. Molecular basis of blood coagulation. In: Hoffman, R., Benz, E.J., Shattil, S.J., Furie, B., Cohen, H.J., Silberstein, L.E., McGlave, P., (Eds.), Hematology: Basic Principles and Practice, 3rd Ed. Churchill Livingstone, London, pp. 1783-1804.

Gir, S., Slack, S., Turitto, V., 1996. A numerical analysis of factor X activation in the presence of tissue factor-factor VIIa complex in a flow reactor. Ann. Biomed. Eng. 24, 394-399.

Goriely, A., Baldwin, A., Secomb, T., 2007. Transient diffusion of albumin in aortic walls: effects of binding to medial elastin layers. Am. J. Physiol. Heart Circ. Physiol. H2195-H2201.

Gornicki, A., 2008. The hemolysis kinetics of psoriatic red blood cells. Blood Cells Mol. Dis. 41, 154-157.

Greenberg, C., Sane, D., Lai, T., 2001. Factor XIII and fibrin stabilization. In: Colman, R., Marder, V., Clowes, A., George, J., Goldhaber, S., (Eds.), Hemostasis and Thrombosis: Basic Principles and Clinical Practice. Lippincott Williams & Wilkins, Baltimore, pp. 317-334.

Guy, R., Fogelson, A., Keener, J., 2007. Fibrin gel formation in a shear flow. Math. Med. Biol. 24, 111-130.

Hockin, M., Jones, K., Everse, S., Mann, K., 2002. A model for the stoichiometric regulation of blood coagulation. J. Biol. Chem. 277 (21), 18322-18333.

Hornyak, T., Bishop, P., Shafer, J., 1989. α-Thrombin-catalyzed activation of human platelet factor XIII: relationship between proteolysis and factor XIIIa activity. Biochem. 28, 7326-7332.

Hwang, C., Edelman, E., 2002. Arterial ultrastructure influences transport of locally delivered drugs. Circ. Res. 90, 826-832.

Inbal, A., Dardik, R., 2006. Role of coagulation factor XIII (FXIII) in angiogenesis and tissue repair. J. Pathophys. Haemost. Thromb. 35 (1-2), 162-165.

Khanin, M., Semenov, V., 1989. A mathematical model of the kinetics of blood coagulation. J. Theor. Biol. 136, 127-134.

Kim, P., Stewart, R., Lipson, S., Nesheim, M., 2007. The relative kinetics of clotting and lysis provide a biochemical rationale for the correlation between elevated fibrinogen and cardiovascular disease. J. Thromb. Haemost. 5, 1250-1256.

Kim, W., Tarbell, J., 1996. Prediction of macromolecular transport through the deformable prous media of an artery wall by pore theory. Korean J. of Chem. Eng. 13 (5), 457-465.

Komotar, R., Zacharia, B., Valhora, R., Mocco, J., Connolly, E., 2007. Advances in vasospasm treatment and prevention. J. Neurol. Sciences. 261, 134-142.

Langille, B., Dajnowiec, D., 2005. Cross-linking vasomotor tone and vascular remodeling: a novel function for tissue transglutaminase? Circ. Res. 96, 9-11.

Lehrer, R., Ganz, T., 2001. Biochemistry and function of monocytes and macrophages. In: Beutler, E., Lichtman, M., Coller, B., Kipps, T., Seligsohn, U. (Eds.), Williams Hematology. Mc-Graw Hill, Columbus, Ohio, pp. 865-872.

Levin, A., Vukmirovic, N., Hwang, C., Edelman, E., 2004. Specific binding to intracellular proteins determines arterial transport properties for rapamycin and paclitaxel. PNAS. 101 (25), 9463-9467.

Lewis, K., Teller, D., Fry, J., Lasser, G., Bishop, P., 1997. Crosslinking kinetics of the human transglutaminase, factor XIII[A_2], acting on fibrin gels and γ-chain peptides. Biochem. 36, 995-1002.

Liu-DeRyke, X., Rhoney, D., 2006. Cerebral vasospasm after aneurysmal subarachnoid hemorrhage: an overview of pharmacologic management. Pharmacother. 26 (2), 182-203.

Lovich, M., Edelman, E., 1999. Tissue concentration of heparin, not administered dose, correlates with the biological response of injured arteries in vivo. PNAS. 96, 11111-11116.

Macfarlane, R., 1964. An enzyme cascade in the blood clotting mechanism, and its function as a biological amplifier. Nature. 202, 498-499.

Martinez-Lemus, L., Hill, M., Bolz, W., Pohl, U., Meininger, G., 2004. Acute machanoadaptation of vascular smooth muscle cells in response to continuous arterial vasoconstriction: implications for functional remodeling. FASEB Journal. 18, 708-710.

McDonagh, R., McDonagh, J., Duckert, F., 1971. The influence of fibrin crosslinking on the kinetics of urokinase-induced clot lysis. Brit. J. Hemat. 21, 323-331.

Murata, K., 1985. Distribution of acidic glycosaminoglycans, lipids and water in normal human cerebral arteries at various ages. Stroke. 16 (4), 687-694.

Nesheim, M., Tracy, R., Tracy, P., Boskovic, D., Mann, K., 1992. Mathematical simulation of prothrombinase. Meth. Enzym. 215, 316-328.

Nielsen, V., 2006. Hemodilution modulates the time of onset and rate of fibrinolysis in human and rabbit plasma. J. Heart Lung Transplant. 25, 1344-1352.

Pico, F., Labreuche, J., Gourfinkel-An, I., Amarenco, P., 2006. Basilar artery diameter and 5-year mortality in patients with stroke. Stroke. 37, 2342-2347.

Ponder, E., 1948. Hemolysis and Related Phenomena. Grune & Stratton, New York.

Pyne-Geithman, G., Morgan, C., Wagner, K., Dulaney, E., Carrozzella, J., Kanter, D., Zuccarello, M., Clark, J., 2005. Bilirubin production and oxidation in CSF of patients with cerebral vasospasm after subarachnoid hemorrhage. J. Cer. Blood Flow & Met. 25, 1070-1077.

Reed, G., Houng, A., 1998. The contribution of activated factor XIII to fibrinolytic resistance in experimental pulmonary embolism. Circ. 99, 299-304.

Reilly, C., Amidei, C., Tolentino, J., Jahromi, B., Macdonald, R., 2004. Clot volume and clearance rate as independent predictors of vasospasm after aneurysmal subarachnoid hemorrhage. J Neurosurg. 101, 255-261.

Rifkind, R., 1965. Heinz body anemia: an ultrastructural study. II. Red cell sequestration and destruction. Blood. 26 (4), 433-448.

Rosen, D., Amidei, C., Tolentino, J., Reilly, C., Macdonald, R., 2007. Subarachnoid clot volume correlates with age, neurological grade, and blood pressure. Neurosurg. 60 (2), 259-267.

Saidel, G., Morris, E., Chisolm, G., 1987. Transport of macromolecules in arterial wall *in vivo*: a mathematical model and analytical solutions. Bull. Math. Biol. 49 (2), 153-169.

Serrador, J., Picot, P., Rutt, B., Shoemaker, J., Bondar, R., 2000. MRI measures of middle cerebral artery diameter in conscious humans during simulated orthostasis. Stroke. 31, 1672-1678.

Siebenlist, K., Meh, D., Mosesson, M., 2001. Protransglutaminase (Factor XIII) mediated crosslinking of fibrinogen and fibrin. Thromb. Haemost. 86, 1221-1228.

Tarbell, J., 2003. Mass transport of arteries and the localization of atherosclerosis. Annu. Rev. Biomed. Eng. 5, 79-118.

Tedgui, A., Lever, M., 1985. The interaction of convection and diffusion in the transport of 131I-Albumin within the media of the rabbit thoracic aorta. Circ. Res. 57, 856-863.

Trumbo, T., Maurer, M., 2003. V341 and V34A substitutions within the factor XIII activation peptide segment (28-41) affect interactions with the thrombin active site. Thromb. Haemost. 89, 647-653.

Truskey, G., Yuan, F., Katz, D., 2004. Transport Phenomena in Biological Systems. Pearson Prentice Hall, New Jersey.

Weisel, J., Nagaswami, C., 1992. Computer modeling of fibrin polymerization kinetics correlated with electron microscope and turbidity observations: clot structure and assembly are kinetically controlled. Biophys. J. 63, 111-128.

Weissberg, H., 1963. Effective diffusion coefficient in porous media. J. Appl. Phys. 34 (9), 2636-2639.

Wootton, D.M., Popel, A.S., Alevriadou, B.R., 2001. An experimental and theoretical study of the dissolution of mural fibrin clots by tissue-type plasminogen activator. Biotechnol Bioeng. 77:405-419.

Young, M., Bell, R., 1980. Estimation of diffusion coefficients of proteins. Biotech. Bioeng. 22, 947-955.

Zimmermann, R., Koenig, J., Zingsem, J., Weisbach, V., Strasswer, E., Ringwald, J., Eckstein, R.,2005. Effect of specimen anticoagulation on the measurement of circulating platelet-derived growth factors. Clinical Chem. 51, 2365-2368.

APPENDIX A

Table 4
Initial concentrations in plasma. The initial concenration of factor XIIIa is determined by the same method as Anand et al., 2008 (i.e. initializing the active factor at a concentration of 0.1% of that of the zymogen). Cross-linked fibrin is not present until factor XIIIa catalyzes the formation of the cross-links from factor Ia.

i	species	initial concentration in plasma (nM)	source
1	IXa	0.09	Anand et al., 2008
2	IX	90	Anand et al., 2008
3	VIIIa	0.0007	Anand et al., 2008
4	VIII	0.7	Anand et al., 2008
5	Va	0.02	Anand et al., 2008
6	V	20	Anand et al., 2008
7	Xa	0.17	Anand et al., 2008
8	X	170	Anand et al., 2008
9	IIa	1.4	Anand et al., 2008
10	II	1400	Anand et al., 2008
11	Ia	7	Anand et al., 2008
12	I	7000	Anand et al., 2008
13	XIa	0.03	Anand et al., 2008
14	XI	30	Anand et al., 2008
15	ATIII	3400	Anand et al., 2008
16	TFPI	2.5	Anand et al., 2008
17	APC	0.06	Anand et al., 2008
18	PC	60	Anand et al., 2008
19	L1AT	45000	Anand et al., 2008
20	tPA	0.08	Anand et al., 2008
21	PLA	2.18	Anand et al., 2008
22	PLS	2180	Anand et al., 2008
23	L2AP	105	Anand et al., 2008
24	XIII	187.5	Furie and Furie, 2000
25	XIIIa	0.1875	n/a
26	cross-linked fibrin	0	n/a

APPENDIX B

Table 5
Code requirements for clot domain.

domain #1: clot	
code requirement	**source**
boundary conditions at x = 0	for i = 1, …, 26, found in Anand et al., 2008
boundary conditions at x = L	for i = 1, …, 26, found in Anand et al., 2008
initial conditions	for i = 1, …, 23, found in Anand et al., 2008 for i = 24,…,26, found in literature search (see Table 4 in Appendix A)
reaction-diffusion equations	for i = 1, …, 23, found in Anand et al., 2008 for i = 24,…,26, found in literature search described in section 2.2: Factor XIII (see Equations 1 - 30)
diffusion coefficients	for i = 1,…,23, found in Anand et al., 2008 for i = 24, 25, calculated using Young and Bell, 1980 method as described in section 2.3: Diffusion through Clot on page 14 for i = 26, diffusion coefficient = 0 (see Table 3 on page 19)

Table 6
Code requirements for arterial wall domain.

	domain #2: arterial wall
code requirement	**source**
boundary conditions at $\hat{x} = 0$	solution from clot domain at x = 0 (output A) (see Figure 7 on page 25)
boundary conditions at $\hat{x} = \hat{L}$	for i = 1,…,25, [i] = 0
initial conditions	for i = 1,…,25, [i] = 0
reaction-diffusion equations	for i = 9, defined by reaction of thrombin with SMCs as explained in section 2.7: Reaction with Wall Components on page 22
diffusion coefficients	for i = 1,…,25, determined by method of Weissberg, 1963 as described in section 2.4: Diffusion through Arterial Wall on page 14 (see Table 3 on page 19)

Table 7
Code requirements for CSF domain.

domain #3:CSF	
code requirement	**source**
boundary conditions at $\tilde{x} = 0$	solution from clot domain at x = L (output B) (see Figure 7 on page 25)
boundary conditions at $\tilde{x} = \tilde{L}$	for i = 1,…,25, [i] = 0
initial conditions	for i = 1,…,25, [i] = 0
reaction-diffusion equations	for i = 1,…,25, no reaction occurs and CSF acts as an infinite sink as described in section 2.5: Diffusion into CSF on page 18
diffusion coefficients	for i = 1,…,25, determined by method of Young and Bell, 1980 as described in section 2.5: Diffusion into CSF (see Table 3 on page 19)

APPENDIX C

Table 8
Kinetic parameters from Anand et al., 2008.

kinetic parameter	reaction	value
k_{11}	XI → XIa	0.0078 min^{-1}
K_{11M}	XI → XIa	50 nM
h_{11A3}	XI → XIa	1.6 x 10-3 nM^{-1} min^{-1}
h_{11L1}	XI → XIa	1.3 x 10-5 nM^{-1} min^{-1}
k_9	IX → IXa	11 min^{-1}
K_{9M}	IX → IXa	160 nM
h_9	IX → IXa	0.0162 nM^{-1} min^{-1}
k_8	VIII → VIIIa	194.4 min^{-1}
K_{8M}	VIII → VIIIa	112000 nM
h_8	VIII → VIIIa	0.222 min^{-1}
h_{C8}	VIII → VIIIa	10.2 min^{-1}
H_{C8M}	VIII → VIIIa	140.5 nM
K_{dZ}	Z (tenase)	0.56 nM
k_5	V → Va	27.0 min^{-1}
K_{5M}	V → Va	140.5 nM
h_5	V → Va	0.17 min^{-1}
h_{C5}	V → Va	10.2 min^{-1}
H_{C5M}	V → Va	14.6 nM
k_{10}	X → Xa	2391 min^{-1}
K_{10M}	X → Xa	160 nM
h_{10}	X → Xa	0.347 nM^{-1} min^{-1}
h_{TFPI}	X → Xa	0.48 nM^{-1} min^{-1}
K_{dW}	W (prothrombinase)	0.1 nM
k_2	II → IIa	1344 min^{-1}
K_{2M}	II → IIa	1060 nM
h_2	II → IIa	0.714 nM^{-1} min^{-1}
k_{PC}	PC → APC	39 min^{-1}
K_{PCM}	PC → APC	3190 nM
h_{PC}	PC → APC	6.6 x 10-7 nM^{-1} min^{-1}
k_1	I → Ia	3540 min^{-1}
K_{1m}	I → Ia	3160 nM

kinetic parameter	reaction	value
h_1	I → Ia	1500 min^{-1}
H_{1m}	I → Ia	250000 nM
k_{PLA}	PLA → PLS	12 min^{-1}
K_{PLAm}	PLA → PLS	18 nM
h_{PLA}	PLA → PLS	0.096 nM^{-1} min^{-1}

APPENDIX D

```
%%%%%%%%%%%%%%%%%%%%%%%%%%%%%%%%%%%%%%%%%%%%%%%%%%%%%%%%%%%%%%%%
%%%%%%%%%%%%%%%%%%%%%%%%%%%%%%%%%%%%%%%%%%%%%%%%%%%%%%%%%%%%%%%%

% deg.m
% degradation of fibrin
% use with myfun.m

clear;clc;close all;

% data recreated from Wootton, 2001, Figure 3
time = [0,3,6,9,12,15,18,21,24,27,30,33,36,39];
loss = [0,0.005,0.01,0.03,0.1,0.18,0.26,0.39,0.5,0.59,0.68,0.76,0.8,0.85];
% fibrin loss (relative to 1)
% at 4 dyn/cm^2 shear

lb = []; % must pass empty lower bounds matrix to define options
ub = []; % must pass empty upper bounds matrix to define options
options = optimset('MaxFunEvals',1000,'TolFun',.00001);
x0 = [1;1;1;1;5;0]; % initial guess of parameters
[x,resnorm] = lsqcurvefit(@myfun, x0,time,loss,lb,ub,options)

mod = x(1)./(x(2) + x(3)*exp(-x(4).*(time+x(5)))) + x(6);

plot(time,loss,'*',time,mod,'o')
xlabel('time (minutes)')
ylabel('Fibrin Loss')
legend('experimental','predicted','Location','NorthWest')
axis([0 40 0 1.0])

a = x(1); b = x(2); g = x(3); h = x(4); k = x(5); m = x(6);
syms indep
est = a/(b + g*exp(-h*indep + k)) + m;
first = diff(est);
second = diff(first);
second = vpa(second,5);
pretty(second)


%%%%%%%%%%%%%%%%%%%%%%%%%%%%%%%%%%%%%%%%%%%%%%%%%%%%%%%%%%%%%%%%

% for use with def.m
% myfun.m
```

```
function F = myfun(x,t)

F = x(1)./(x(2) + x(3)*exp(-x(4)*(t+x(5)))) + x(6);

%%%%%%%%%%%%%%%%%%%%%%%%%%%%%%%%%%%%%%%%%%%%%%%%%%%%%%%%%%%%%%%%
%%%%%%%%%%%%%%%%%%%%%%%%%%%%%%%%%%%%%%%%%%%%%%%%%%%%%%%%%%%%%%%%

% kl.m
% Fibrinogen (I) -> Fibrin (Ia)
% use with myfun.m

clear;clc;close all;

% data recreated from Weisel, 1992, Figure 2
time = linspace(0,300,7)./60;
clot = [0,0.23,0.65,0.80,0.85,0.89,0.95];
% fraction of mature fibrin

lb = []; % must pass empty matrix of lower bounds to define options
ub = []; % must pass empty matrix of upper bounds to define options
options = optimset('MaxFunEvals',1000,'TolFun',.00001);
x0 = [0;1;1;1]; % initial guess of parameters
[x,resnorm] = lsqcurvefit(@myfun, x0,time,clot,lb,ub,options)

mod = x(1) + x(2)*exp(x(3)*time.^x(4));

plot(time,clot,'*',time,mod,'o')
xlabel('time (minutes)')
ylabel('fraction of activated fibrin (I)')
legend('experimental','predicted','Location','East')
axis([0 5 0 1])

syms indep
est = x(1) + x(2)*exp(x(3)*indep^x(4));
first = diff(est);
first = vpa(first,4)
pretty(first);

%%%%%%%%%%%%%%%%%%%%%%%%%%%%%%%%%%%%%%%%%%%%%%%%%%%%%%%%%%%%%%%%

% myfun.m
% for use with kl.m

function F = myfun(x,t)
```

```
F = x(1) + x(2).*exp(x(3).*t.^x(4));

%%%%%%%%%%%%%%%%%%%%%%%%%%%%%%%%%%%%%%%%%%%%%%%%%%%%%%%%%%%%%%%%
%%%%%%%%%%%%%%%%%%%%%%%%%%%%%%%%%%%%%%%%%%%%%%%%%%%%%%%%%%%%%%%%

% k2.m
% Fibrin (I) -> crosslinked fibrin (Iac)
% for use with myfun.m

clear;clc;close all;

% data recreated from Siebenlist, 2001, Figure 4
time = [1,5,10,15,20,25,30,35,40,45,50,55,60,90];
insol = [0,58,80,82,84,86,88,89,90,91,92,93,94,95];
% percent insoluble fibrin (Iac)

lb = []; % must pass empty matrix of lower bounds to define options
ub = []; % must pass empty matrix of upper bounds to define options
options = optimset('MaxFunEvals',1000,'TolFun',.00001);
x0 = [0;100;.5;.5]; % initial parameter guess
[x,resnorm] = lsqcurvefit(@myfun, x0,time,insol,lb,ub,options)

mod = x(1) + x(2)*exp(x(3)*time.^x(4));

plot(time,insol,'*',time,mod,'o')
xlabel('time (minutes)')
ylabel('percent insoluble fibrin')
legend('experimental','predicted','Location','East')
axis([0 90 0 100])

syms indep
est = x(1) + x(2)*exp(x(3)*indep^x(4));
first = diff(est);
first = vpa(first,4)
pretty(first);

%%%%%%%%%%%%%%%%%%%%%%%%%%%%%%%%%%%%%%%%%%%%%%%%%%%%%%%%%%%%%%%%

% myfun.m
% for use with k2.m

function F = myfun(x,t)
```

```
F = x(1) + x(2)*exp(x(3)*t.^x(4));

%%%%%%%%%%%%%%%%%%%%%%%%%%%%%%%%%%%%%%%%%%
%%%%%%%%%%%%%%%%%%%%%%%%%%%%%%%%%%%%%%%%%%
```

VITA

Name:	Erin Kathleen Hackney
Address:	337 Zachry Engineering Center 3120 TAMU College Station, TX 77843-3120
Email Address:	erkjohnson@gmail.com
Education:	B.S., Biomedical Engineering, Texas A&M University, 2007 M.S., Biomedical Engineering, Texas A&M University, 2009